International Journal of Applied Pharmaceutics

ISSN- 0975-7058 Vol 16, Issue 6, 2024

Original Article

TRANSETHOSOMES FOR ENHANCED TRANSDERMAL DELIVERY OF METHOTREXATE AGAINST RHEUMATOID ARTHRITIS: FORMULATION, OPTIMISATION AND CHARACTERISATION

POOJARI PRATIKSHA N.[1], SNEH PRIYA[1*], SANJANA[1], PRASANNA SHAMA KHANDIGE[2]

Nitte (Deemed to be University), NGSM Institute of Pharmaceutical Sciences (NGSMIPS), Department of Pharmaceutics, Mangalore, India
[*]Corresponding author: Sneh Priya; [*]Email: snehpriya123@nitte.edu.in

Received: 13 Jun 2024, Revised and Accepted: 13 Sep 2024

ABSTRACT

Objective: The study aimed to develop and optimise Methotrexate (MTX)-loaded Transethosomal Film-Forming Gel (TE FFG) for transdermal delivery to treat rheumatoid arthritis while alleviating the side associated with oral administration.

Methods: The Transethosomes (TE) were prepared using the thin film hydration technique and incorporated into an FFG using chitosan. The Box-Behnken Design method was used to analyse the influence of independent variables such as the concentration of soya lecithin, surfactant, and ethanol on parameters including vesicle size, PDI (Polydispersity Index), zeta potential, and entrapment efficiency. The optimised transethosomal suspension was incorporated into the FFG using 3% chitosan and other excipients. *In vitro* drug release and *ex vivo* skin permeation of FFG were performed using Franz diffusion cells.

Results: The vesicle size, PDI, zeta potential and entrapment efficiency of the optimised formulation of TE were 110.3 nm, 0.352,-14.4 mV and 49.36%, respectively. The Transmission Electron Microscopy (TEM) image showed that the vesicles were uniform and spherical. The *in vitro* drug release study was higher for Conventional (CL) FFG) than TE FFG and the drug release mechanism was fitted into the Higuchi model. The permeation was higher for TE FFG, with the steady-state flux being 1.55 times greater than the CL FFG. The skin irritation test on Wistar rats revealed no indication of irritation on the skin. The histopathology examination showed a significant reduction in the inflammatory cells in the treated group.

Conclusion: Therefore, the results concluded that the formulated MTX-loaded TE FFG could be a potentially promising substitute for the oral delivery of methotrexate

Keywords: Methotrexate, Rheumatoid arthritis, Transethosomes, Box behnken design, Film-forming gel

DOI: https://dx.doi.org/10.22159/ijap.2024v16i6.51772 Journal homepage: https://innovareacademics.in/journals/index.php/ijap

INTRODUCTION

A systemic autoimmune disease known as Rheumatoid Arthritis (RA) is characterised by a long-term inflammation process that can harm joints and extra-articular organs like the lung, eye, heart, skin, kidney, digestive system and nervous system [1]. Inflammatory response, bone destruction and chronic synovitis are all associated with this autoimmune disease, along with gradual joint deterioration, deformity and dysfunction followed by complete impairment. The complicated interrelationship between acquired deficits in immune regulation and genetics results in pathological activation of the immune system concerning physiological stimulus and pathogens, other contributing reasons involving diet and environment [2]. Strategies for rheumatoid arthritis treatment include disease-modifying anti-rheumatic drugs like Methotrexate (MTX), hydroxychloroquine sulfasalazine and leflunomide, glucocorticoids, non-steroidal anti-inflammatory drugs and biological agents. Methotrexate is regarded as the frontline standard medication for treating rheumatoid arthritis due to its effectiveness in treatment and relatively low cost [3].

MTX is a drug with immunosuppressant and antineoplastic properties. It treats RA, lymphoma, lymphoblastic leukaemia, psoriasis, osteosarcoma, medulloblastoma, etc. and works as a folic acid antagonist. MTX belongs to the disease-modifying anti-rheumatic drug class with 454.44 Da as molecular weight. The mechanism of action includes competitive inhibition of the enzyme dihydrofolic acid reductase, resulting in the inhibition of the formation of tetrahydrofolate required to synthesise purine nucleotides and thymidine. In rheumatoid arthritis, it is used at lower doses to reduce tenderness and swelling associated with the disease [4, 5]. MTX belongs to class IV of the BCS classification, which states the drug is low aqueous soluble and poorly permeable. The effectiveness of MTX is frequently hindered due to short half-life, side effects and decreased bioavailability due to low permeability and water solubility [6-8].

Transdermal drug delivery can be a choice for drug candidates that lead to toxicity or side effects when administered orally. Transdermal delivery is considered in many ways over the conventional dosage. Some of the benefits include increased bioavailability by the elimination of first-pass metabolism and drug degradation by enzymes of the GI tract. It offers sustained and controlled drug administration and prevents the potential hazards associated with IV therapy. Also, patient compliance is enhanced due to reduced frequency of dosing. The risk or trauma of infection is reduced due to the non-invasive mode of delivery [9].

Phospholipid-based carriers for drug delivery have been a popular approach for effective percutaneous administration due to their biodegradable and biocompatible nature. The barrier function of the stratum corneum impedes the penetration of medication through the skin [10]. For this purpose, liposomes were opted as an approach for transdermal delivery. Liposomes are phospholipid (PC) vesicles with an aqueous section encapsulated by one or more lipid bilayers [11]. However, the liposomes accumulated in the epidermal layer due to a lack of flexibility to enter the innermost layers. The penetration issue was later resolved by discovering deformable liposomes with improved flexibility. These deformable liposomes include phospholipids and water, along with edge activators. Transferosomes, a novel class of liposomes made of a phospholipid bilayer and a surfactant, were developed as a drug delivery system. The surfactant provides the elasticity of the vesicles. The affinity and biocompatibility of the transethosomal vesicles with stratum corneum are granted by phospholipids.

The penetration of vesicles is enhanced using a higher concentration of ethanol, which acts as a penetration enhancer. Ethanol also acts by preventing wound infections [12]. The hydrophilic and hydrophobic parts of transferosomes can encapsulate various drugs with varying solubility. Penetration of vesicles is enhanced by their ability to deform their structure and penetrate through narrow constrictions [13, 14]. Transethosomes (TEs) comprise the benefits of both ethosomes and transferosomes. They are characterised by high vesicle elasticity, which improves the skin permeation of the transethosomal formulation by rearrangement of the vesicular lipid

bilayer. This characteristic is due to the synergistic action of ethanol and edge activator [15-17].

Therefore, the present study aimed to formulate the Transethosomal Film-Forming Gel (TE FFG) containing MTX for enhancing transdermal delivery of the drug and to reduce the adverse effects typically associated with oral intake of the drug for the treatment of RA.

MATERIALS AND METHODS

Chemicals and reagents

MTX was procured from Yarrow Chem Products, Mumbai. Soya Lecithin was obtained from Hi Media Laboratories, Mumbai. Tween 80, Ethanol, Propylene glycol, Oleic acid was obtained from Loba chemie, Mumbai. Chitosan and Complete Freund's adjuvant was procured from Sigma Aldrich Chemicals Pvt Ltd, Bengaluru.

Formulation and characterisation of MTX-loaded TEs

Design of experiments

Design of Experiments (DoE) is a primary statistical tool for implementing Quality by Design in research and industrial fields [18]. It offers a systematic methodology for designing and executing experiments to extract maximum information [19, 20]. This organised approach utilises mathematical models to establish correlations between input factors (independent variables) that affect one or more output responses (dependent variables) [21]. In the context of this study, the literature survey suggested three independent variables: concentration of soya lecithin (A), surfactant (B) and ethanol (C) and their effects were evaluated on four dependent variables: vesicles size, PDI, zeta potential and entrapment efficiency of TEs. The optimisation of the transethosomal formulation was carried out using the Box-Behnken Design, facilitated by Design Expert ® software (version 13.0.15, Stat-Ease, Inc. Minneapolis, MN, USA). The transethosomal formulation was prepared by varying the concentration of soya lecithin (g), surfactant (µl) and ethanol (%) at different levels within the range of 1-2%, 0.2-0.4% and 20-30%, respectively. The software analysed the influence of these individual factors and their combined effect on dependent variables such as vesicle size (nm), PDI, zeta potential (mV), and entrapment efficiency (%). The experimental design encompassed 17 formulation runs, as outlined in table 1.

Preparation of TEs

MTX-loaded TE was prepared using the thin-film hydration method as per table 1. A ratio of 2:1 of chloroform and methanol was employed to dissolve the phospholipid. The resulting mixture was placed in a round-bottom flask, where the organic phase was evaporated using a rotary evaporator until a thin film was obtained. This evaporation process occurred at a temperature of 40 °C under reduced pressure conditions. Subsequently, the thin film was hydrated using the aqueous phase, which consisted of the drug, Tween 80, and ethanol dissolved in 20 ml of phosphate buffer solution at pH 7.4. The hydrated suspension was then transferred to a rotary shaker and subjected to sonication using a probe sonicator to reduce the size of the particles [22].

Characterisation of MTX-loaded TEs

Vesicle size, size distribution and zeta potential

The vesicle size, size distribution and zeta potential of TEs were analysed using a zeta sizer equipped with dynamic light scattering (Nano ZS, Malvern Instruments, UK). The zeta potential of a particle denotes the net electrical charge it accumulates within a specific medium. This value is crucial for assessing the stability of the formulation [23].

Percentage entrapment efficiency

Transethosomal suspension of about 10 ml was transfered in a 15 ml Tarsus centrifuge tube, which was centrifuged by cold centrifugation at 4 °C for 30 min at 12,000 rpm. The high-speed centrifugation causes the separation of the suspension, leading to a supernatant and a sediment layer. A UV spectrophotometer was employed in order to analyse the concentration of MTX present in the supernatant at 303 nm, and the concentration was calculated as follows [24].

$$\%\ \text{Entrapment efficiency} = \frac{\text{Total amount of drug} - \text{Amount of unentrapped drug}}{\text{Total amount of drug}} \text{X } 100$$

Formulation and characterisation of an optimised batch of TEs

Design-Expert version 13 software was used to develop and optimise the parameters for the formulation. It was used to assess the impact of process variables on the responses. This software facilitated the assessment of the impact of process variables on the responses, aiding in the optimisation process. The optimisation of TEs was carried out based on specific constraints, including minimum particle size, minimum PDI, optimum zeta potential, and maximum entrapment efficiency. The software generated a solution with good desirability (0.924), selected as an optimised formulation. The optimised formulation was prepared as per the software's solution: 2%w/v of soya lecithin, 0.302% v/v of tween 80 and 20% of ethanol. The prepared formulation was evaluated for various parameters like vesicle size, size distribution, zeta potential, and percent entrapment efficiency.

Transmission Electron Microscopy (TEM)

The morphology of the MTX-loaded TE vesicles was observed by transmission electron microscope. The optimised transethosomal suspension was diluted ten-fold, and the drop was left for a minute by placing it on the 300-mesh carbon-coated copper grid. It allows some of the vesicles to settle on the carbon substrate. The filter paper was utilised to remove excess dispersion from the grid and rinsed twice for 3-5 seconds with distilled water. Then, the sample was examined under a microscope [25, 26].

Elasticity test

The elasticity study assesses the deformability index of TEs as a unique parameter that differentiates it from liposomes. This test was performed using the extrusion technique with a polycarbonate membrane.

$$D = \frac{J}{t}\left(\frac{r_v}{r_p}\right)^2$$

Where D-deformability index (ml/s), J-the amount of dispersion extruded (ml), t-extrusion time (s), r_v-vesicle size after extrusion (nm), r_p-pore size of the extrusion membrane (nm) [27].

Formulation and characterisation of FFG

The 1% MTX-loaded TE FFG and Conventional (CL) FFG were formulated by using 3% chitosan in distilled water. The required volume of optimised transethosomal suspension and the pure drug, respectively, was added to the chitosan solution and homogenised for 5 min. Later, 2% propylene glycol, oleic acid and 40% ethanol were added with continuous mixing. At last, 4% lactic acid was added for the required viscosity.

Physical appearance, pH, viscosity, spreadability

The physical characteristics of the FFG were visually evaluated [28]. 1g of the FFG was weighed and diluted with 100 ml of distilled water. The pH of the resulting solution was measured using an electronic pH meter after allowing it to equilibrate for 1 minute [29]. The FFG was assessed for viscosity using Brookfield Viscometer DV-II+PRO, D220. The viscosity was examined for 0.5, 1, 2, 2.5 and 3 rpm using spindle number T-96 [30]. 0.5 g of the FFG was used to determine the spreadability, and it was placed between two 20 cm x 20 cm smooth surfaced tiles. After placing the gel on one of the tiles, the initial diameter of the placed gel was recorded in centimetres. Subsequently, another glass plate weighing 200 gs with identical dimensions was placed over the gel for 1 minute, after which the upper plate was lifted, and the diameter of the spread gel was measured [31, 32].

Drug content

The drug content was examined by dissolving 1g of the FFG in 100 ml of phosphate buffer solution pH 7.4 in a volumetric flask,

resulting in a 100µg/ml concentration of the solution. From the above solution, 0.5 ml was pipetted out and further diluted up to 10 ml in the volumetric flask using a phosphate buffer solution of pH 7.4. The drug was estimated using a UV spectrophotometer at a wavelength of 303 nm after filtration.

Drug-excipient compatibility study by Fourier Transform Infrared Spectroscopy (FTIR)

To find the chemical interaction between the drug and excipients, an FTIR spectra matching approach was performed by using an FTIR spectrometer (Bruker Alpha II FTIR, Japan). The spectrum was acquired using the attenuated total reflectance (ATR) method, wherein a slight quantity of the sample was positioned beneath the probe of FTIR spectrophotometer. The probe was securely fastened, and scanning was performed in the range of 4000–500 cm^{-1} to capture the spectra of the samples. FTIR spectra of the TE and TE FFG were recorded, and the presence of principal peaks was compared with drug spectra.

***In vitro* drug release study**

The *in vitro* drug release study for transethosomal suspension was conducted using a single-cell diffusion apparatus. The diffusion membrane was soaked overnight in a phosphate buffer of pH 7.4. Subsequently, the membrane was wrapped under the donor compartment, over which the CL and TE FFG equivalent to 10 mg were introduced. The receptor compartment was filled with a phosphate buffer solution of pH 7.4, and surrounded by a water jacket. The apparatus was placed on a magnetic stirrer set at 150 rpm, with a small magnetic bar and optimum temperature. Samples were withdrawn from the sampling port at regular intervals of 0.25, 0.5, 1, 2, 3, 4, 5, 6, 7, 8, 9, 10, 12, and 24 h. A volume of 3 ml of the sample was withdrawn from the receptor compartment at each interval, with an equal volume of fresh phosphate buffer solution being replaced to maintain sink conditions. The withdrawn samples were measured spectrophotometrically at 303 nm [33].

Different models were utilised to analyse the drug release kinetics of formulation. The data collected from the drug release study was plotted according to each model, including zero-order kinetics (cumulative percentage drug release vs time) and first-order (log cumulative percentage unreleased vs time). Korsmeyer Peppas model (log cumulative percentage drug release vs time) and Higuchi model (cumulative percentage drug release vs square root of time) are mathematical models used to detect the mechanism of drug release and release of drugs from various matrix systems, respectively [34].

***Ex vivo* skin permeation studies of FFG using goat skin**

The ex vivo skin permeation study was performed through goat skin. The goat skin was procured from a slaughterhouse and thoroughly cleaned to achieve hairless skin before being stored in phosphate buffer pH 7.4. The study was performed on the Franz diffusion apparatus, consisting of the donor and acceptor compartments. The skin is attached to the donor compartment. CL FFG or TE FFG containing a drug equivalent to 10 mg were applied onto the dermal layer of skin in the donor compartment. The acceptor compartment contained 12 ml of phosphate buffer pH 7.4 and a small magnetic bead for stirring. The study continued for 24 h at 37±0.5 °C, with magnetic stirring at 50 rpm. 1 ml of the sample was withdrawn from the acceptor compartment at regular intervals, and the same volume of fresh phosphate buffer of pH 7.4 was replaced to maintain the sink condition. The withdrawn sample was appropriately diluted and analysed spectrophotometrically by obtaining the absorbance at 303 nm.

***In vivo* skin irritation study**

The FFG was evaluated for a skin irritation test conducted on Wistar rats. It was performed to assess the degree of skin irritation caused by the formulation, enabling the selection of the best formulation with minimal irritation. The animal study was approved by the Institutional Animal Ethics Committee of NGSM Institute of Pharmaceutical Sciences under the protocol approval number NGSMIPS/IAEC/AUG-2023/380. The animals were procured from Nitte Center for Animal Research and Experimentation Mangalore and were cleaned and made fur-free at the dorsal side using a hair removal cream after anesthetising them. Hair removal of rats was done 24 h prior so that any sensitivity from hair removal could be avoided. The gels were applied to the back of the rats on the following day. The blank FFG was used in the control group, whereas MXT-loaded TE FFG was applied to the test group animal. The test material was removed after 24 h, and the surface of the skin was rinsed with distilled water; subsequently, the skin was observed at 24 h for any sign of erythema or edema [35, 36].

The anti-rheumatic activity of MTX-loaded TE FFG

Complete freund's adjuvant (CFA) induced arthritis

Arthritis was induced intraperitoneally by injecting 0.1 ml (0.1% w/v) CFA suspension into the rats. By injecting 0.1 ml of CFA suspension, arthritis was induced in each rat, except for the normal control group. It usually takes 7-9 d for the arthritis to develop.

The animals were divided into the following groups:

Group 1: Normal control group (rats without inducing disease)

Group 2: Disease control group (Rats will be treated with CFA)

Group 3: Rats will be treated with the Blank TE FFG after CFA administration.

Group 4: Rats will be treated with an MTX-marketed gel after CFA administration

Group 5: Rats will be treated with MTX-loaded TE FFG after CFA administration.

Physical parameters

To assess the systemic inflammation associated with arthritis, paw thickness and body weight was checked. The experiment rats' body weight and paw diameter were recorded using the weighing balance and digital vernier calliper, respectively, before inducing CFA and on days 7^{th}, 14^{th} and 21^{st} following CFA injection.

Statistical analysis

A statistical analysis was conducted using graph pad in stat demo. The experimental data was presented as mean±standard deviation. Differences between groups were compared using one-way ANOVA followed by Tukey's test. A p-value of<0.05 was considered as the level of significance.

Histopathology

On the 22^{nd} d of the study, the rats were anaesthetised and subsequently sacrificed. The ankle joints of the rats were then dissected for histopathological analysis. The sections were fixed in a 10% formalin solution, followed by sectioning. These sections were stained using hematoxylin and eosin to examine the histopathological changes in the rats throughout the study [37, 38].

RESULTS AND DISCUSSION

Formulation and characterisation of MTX-loaded TEs

The MTX-loaded TEs were synthesised using the thin-film hydration method. The box-Behnken design was employed to optimise the formulation. The impact of independent variables, including the concentration of soya lecithin, surfactant, and ethanol, on dependent variables such as particle size, PDI, zeta potential, and entrapment efficiency was assessed. It was observed that the selected factors significantly affected all of the investigated responses.

Vesicle size of TEs

The vesicle size significantly influences the penetration of TEs through the skin, and hence, a vesicle size<200 nm is desirable, as per the literature. The independent variables, the concentration of soya lecithin and ethanol, significantly affected vesicle size. In contrast, the surfactant concentration had no considerable impact on vesicle size, as shown in table 1, fig. 1(A) and 2(A). An increase in soya lecithin concentration from 1% to 2%w/v resulted in a gradual increase in vesicle size. It might be attributed to the increase in the thickness of lipid bilayers and viscosity of the TEs as the lipid content is raised, thereby increasing the vesicle size [39].

Moreover, as the concentration of ethanol increases from 20% to 30% v/v, the vesicle size also increases. This increase may be attributed to the penetration of ethanol molecules into the lipid bilayer, causing an increase in spacing between the lipid molecules and resulting in the swelling of vesicles. However, no change in vesicle size was observed when the concentration of Tween 80 increased from 0.2% to 0.4%v/v. As shown in table 2, the model generated for vesicle size had a p-value of<0.0001 and an F-value of 40.78, indicating the model to be significant. The F-value of 0.15 implies that the lack of fit is not significant. The predicted R^2 of 0.8701 is in reasonable agreement with the adjusted R^2 of 0.8818; the difference is less than 0.2.

Vesicle size =+157.08+13.15(A)*+1.62(B)+55.57(C)*

Where A is the concentration of soya lecithin, B is the concentration of Tween 80, and C is the concentration of ethanol, the coefficient in this equation reflects the standardised beta coefficient, and the asterisk symbol implies variable significance as shown in table 2. A positive sign represents a synergistic effect.

PDI of TEs

PDI indicates the unimodal distribution of the vesicle size, providing insight into the degree of homogeneity or heterogeneity within the formulation. A low PDI indicates a narrow-sized distribution, and a PDI near 1 indicates a broader-sized distribution. The ethanol concentration showed a significant effect on PDI, as depicted in table 1, fig. 1(B) and fig. 2(B). An increase in the concentration of soya lecithin from 1 to 2% resulted in a gradual decrease in PDI, although this change was not significant. Similarly, as the surfactant concentration increased from 0.2 to 0.4%, there was a gradual decrease in PDI, which was also insignificant. This decrease may be due to the high concentration of soya lecithin, which favours particle uniformity with an increase in temperature during the thin film hydration process, causing enhanced fluidity of the bilayer [40]. Additionally, an increase in the surfactant concentration from 0.2 to 0.4% led to a gradual decrease in PDI, which may be attributed to the reduction in interfacial tension between the lipid and aqueous phase, facilitating uniform-sized vesicles. An increase in ethanol concentration from 20 to 30% caused an increase in PDI.

The model generated for PDI exhibited a p-value of 0.0001 and F-value of 16.01, indicating the linear model to be significant. The F-value of 1.51 suggests the lack of fit is not significant. The predicted R^2 of 0.6083 is in reasonable agreement with the Adjusted R^2 of 0.7378, with a difference being less than 0.2, as shown in table 2. The polynomial equation obtained from the results of the analysis is as follows:

PDI=+0.4535-0.0145(A)-0.0220(B)+1140(C)*

Where A is the concentration of soya lecithin, B is the concentration of Tween 80, and C is the concentration of ethanol, the coefficient in this equation reflects the standardised beta coefficient, and the asterisk symbol implies variable significance, as shown in table 2.

Zeta potential of TEs

Zeta potential serves as an indicator of the stability of the formulation. When particles possess similar charges, repulsion occurs, thereby reducing the aggregation of vesicles and enhancing the stability of the formulation. The concentration of soya lecithin, surfactant, and ethanol significantly affected zeta potential, as depicted in table 2, fig. 1(C), and fig. 2(C). An increase in soya lecithin concentration from 1 to 2% resulted in a significant initial reduction in zeta potential, followed by a gradual increase. This reduction is attributed to the negatively charged components of soya lecithin [41].

Similarly, an increase in surfactant concentration from 0.2% to 0.4% led to a slight initial decrease in zeta potential, followed by a rapid rise. The rapid increase is due to the non-ionic surfactant, which gets adsorbed onto the vesicle surface, causing a reduction in the overall charge of the vesicles. Moreover, the concentration of ethanol from 20 to 30% had no significant effect initially but later showed a rapid increase in zeta potential.

The model generated for zeta potential has a p-value of 0.0001 and an F-value of 26.09, indicating the quadratic model to be significant. Additionally, the lack of fit (F-value of 1.11) suggests that the lack of fit is not significant. The predicted R^2 of 0.7645 is in reasonable agreement with the adjusted R^2 of 0.9338, with a difference of less than 0.2. The polynomial equation obtained from the results of the analysis is as follows:

Zeta Potential =-17.23-2.36(A)*+1.16(B)*+2.37(C)*-3.18(AB)* 1.90(AC)*+4.20(BC)*+2.42(A^2)*+5.38(B^2)*+2.77(C^2)*

Where A is the concentration of soya lecithin, B is the concentration of Tween 80, and C is the concentration of ethanol. The coefficient in the equation reflects the standardised beta coefficient, and the asterisk symbol indicates variable significance, as depicted in table 2.

Percentage entrapment efficiency

The concentration of Soya Lecithin, Tween 80 and ethanol demonstrated a significant effect on entrapment, as illustrated in table 2, fig. 1(D) and 2(D). Increasing the concentration of soya lecithin from 1 to 2% initially led to a decrease in %EE, followed by a rapid increase. This rapid increase in entrapment efficiency may be attributed to the enhancement of lipid viscosity resulting from the increase in lipid concentration. This increase in viscosity can prevent leaching of the drug from the lipid bilayer due to increased hydrophobicity and lengthening of the alkyl chain [39]. The concentration of surfactant from 0.2 to 0.4% caused a significant increase in Entrapment efficiency. This is because Tween 80 can stabilise the vesicle structure, prevent leakage of encapsulated materials, and improve the encapsulation process [23]. Further, the entrapment efficiency gradually increased with the initial increase in ethanol concentration, followed by a gradual decrease. This phenomenon could be attributed to the fact that an increase in ethanol concentration leads to higher fluidity of the vesicles, causing the drug to leak out [42].

The model generated for entrapment efficiency exhibited a p-value of<0.0001 and F-an F-value of 61.77, indicating that the model is significant. The F-value of 2.67 indicates the Lack of fit is not significant. The predicted R^2 of 0.8608 is in reasonable agreement with the adjusted R^2 of 0.9716, with a difference of less than 0.2. The polynomial equation derived from the analysis is as follows:

%EE=+39.45+4.88(A)*+8.78(B)*+1.33(C)*+2.48(AB)*- 1.45(AC)+2.30(BC)*+7.79(A^2)*-0.3430(B^2)-1.94(C^2)*

The coefficient in this equation reflects the standardised beta coefficient, and the asterisk symbol implies variable significance, as shown in table 2.

Formulation and characterisation of optimised batch

The constraints like minimum particle size, minimum PDI, optimum zeta potential (-15mV) and maximum entrapment efficiency were considered. Based on the solution provided by the software, the optimised formula was prepared, consisting of 2%w/v soya lecithin, 0.302%v/v surfactant and 20%v/v ethanol. The observed values of vesicle size, PDI, zeta potential and entrapment efficiency were 110.3 nm, 0.352,-14.4mV, and 49.36%, respectively, as shown in fig. 3. The percentage error was less than ±5% of the predicted value, which is acceptable.

Transmission electron microscopy

TEM images revealed the surface morphology of vesicles, exhibiting the unilamellar vesicular structure provided in fig. 4. The TEM image supports the result obtained by the Malvern zeta sizer for the optimised transethosomal formulation, depicting the size range of 115 nm, close to the size detected by the zeta sizer.

Table 1: Results of the response of TEs as per box behnken design

Form code	Variables			Response			
	Soya lecithin %w/v	Tween 80 %v/v	Ethanol %v/v	*Vesicle size±SD (nm) Y1	*PDI±SD Y2	*ZP±SD Y3	*EE±SD (%) Y4
1	1	0.2	25	134.23±8.91	0.514±0.085	-10.36±0.50	35.93±1.25
2	2	0.2	25	170.73±4.20	0.419±0.020	-9.65±1.42	42.01±2.45
3	1	0.4	25	141.13±3.47	0.467±0.019	-2.86±0.47	46.83±2.56
4	2	0.4	25	179.7±4.37	0.459±0.017	-14.86±2.67	62.83±1.43
5	1	0.3	20	97.36±5.44	0.373±0.016	-14.8±5.63	38.56±2.43
6	2	0.3	20	107.03±5.84	0.324±0.019	-14.8±3.21	49.96±1.76
7	1	0.3	30	208.76±16.90	0.523± 0.018	-5.49±1.70	43.56±2.98
8	2	0.3	30	229.26±4.98	0.559±0.010	-13.08±0.17	49.14±2.12
9	1.5	0.2	20	99.06±4.13	0.331±0.015	-8.63±2.75	28.24±1.54
10	1.5	0.4	20	111.63±3.42	0.344±0.037	-13.51±2.48	42.88±4.17
11	1.5	0.2	30	218.53±17.04	0.692±0.173	-13.06±2.40	26.85±2.65
12	1.5	0.4	30	203.06±1.30	0.510±0.075	-1.15±1.45	50.7±1.65
13	1.5	0.3	25	159.86±2.66	0.393±0.008	-19.4±2.45	40.91±2.47
14	1.5	0.3	25	115.1±2.51	0.476±0.084	-16.31±6.49	38.25±3.33
15	1.5	0.3	25	170.9±15.44	0.453±0.144	-17.13±0.98	39.58±4.11
16	1.5	0.3	25	154.16±2.34	0.397±0.072	-17.2±0.56	38.5±1.33
17	1.5	0.3	25	169.81±2.45	0.475±0.065	-16.1±0.66	39.99±2.54

*Data is given in mean±SD (N=3)

Table 2: Summary of regression analysis and ANOVA

S. No.	Factor	Vesicle size (Adjusted R^2=0.8818)		PDI (Adjusted R^2=0.7378)		Zeta potential (Adjusted R^2=0.9338)		% EE (Adjusted R^2=0.9716)	
		Est. β	P value	Est. β	P value	Est. β	P value	Est. β	P value
1	Intercept	157.08	<0.0001	0.4535	<0.0001	-17.23	0.0001	39.45	<0.0001
2	A-Soya lecithin	13.15	0.0243	-0.0145	0.4060	-2.36	0.0016	4.88	<0.0001
3	B-Tween 80	1.62	0.7586	-0.0220	0.2152	1.16	0.0435	8.78	<0.0001
4	C-Ethanol	55.57	<0.0001	0.1140	<0.0001	2.37	0.0016	1.33	0.0345
5	AB	-	-	-	-	-3.18	0.0021	2.48	0.0105
6	AC	-	-	-	-	-1.90	0.0253	-1.45	0.0818
7	BC	-	-	-	-	4.20	0.0004	2.30	0.0148
8	A^2	-	-	-	-	2.42	0.0076	7.79	<0.0001
9	B^2	-	-	-	-	5.38	<0.0001	-0.3430	0.6382
10	C^2	-	-	-	-	2.77	0.0039	-1.94	0.0276

Est; Estimated, β: beta coefficient

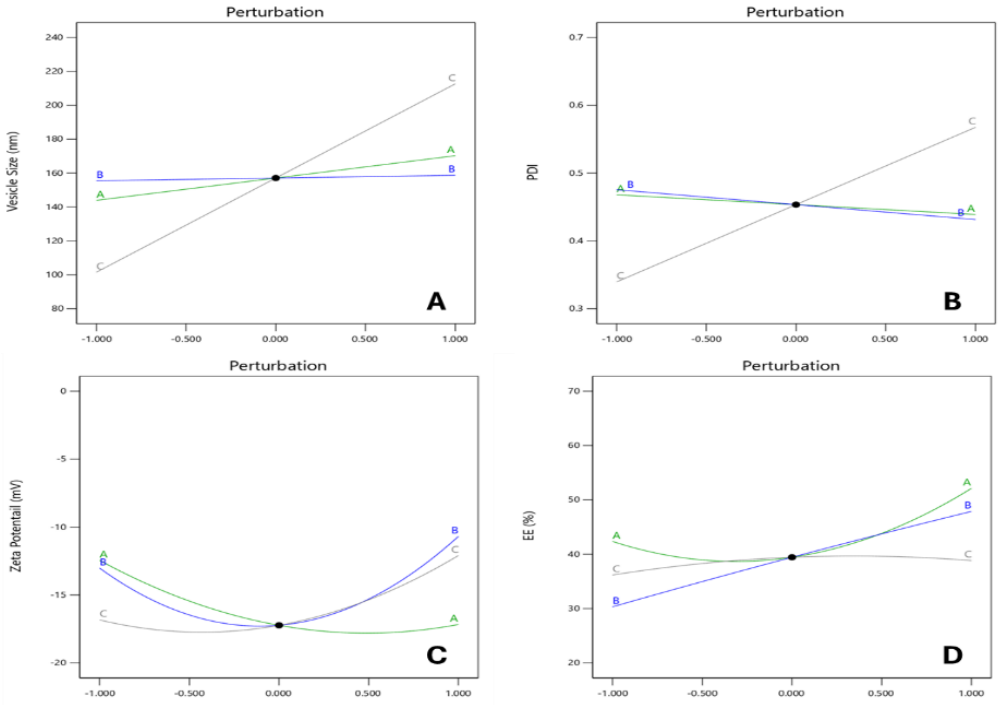

Fig. 1: Perturbation plot representing the effect of soya lecithin, tween 80 and ethanol on A) Vesicle size B) PDI C) Zeta potential D) % entrapment efficiency of TEs

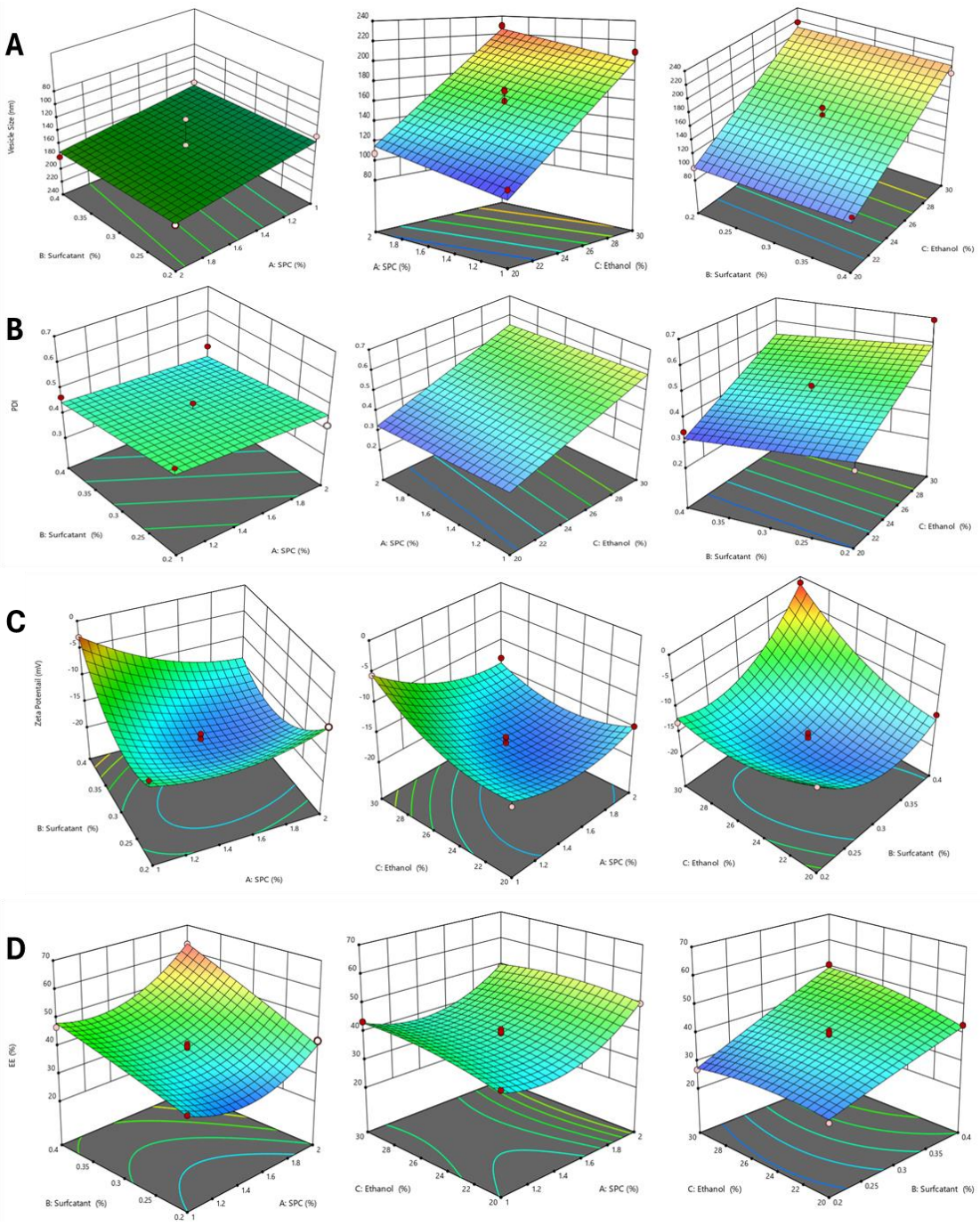

Fig. 2: 3D Response surface curve representing the effect of soya lecithin, tween 80 and ethanol on A) Vesicle size B) PDI C) Zeta potential D) Entrapment efficiency

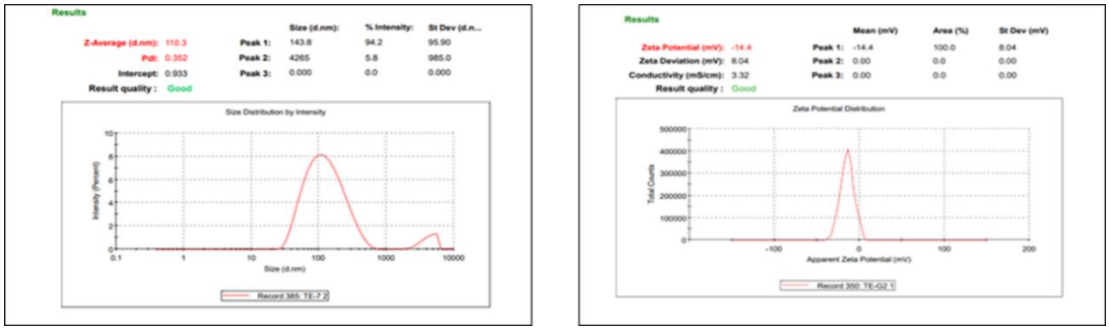

Fig. 3: Size distribution and zeta potential of optimised formulation of TE

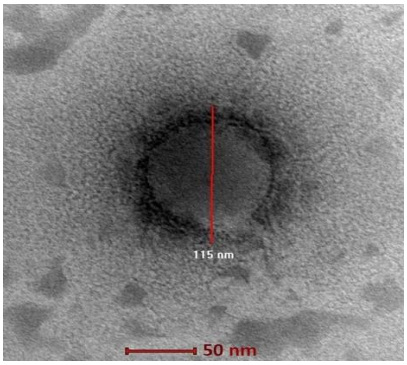

Fig. 4: TEM image of optimised TE at 50 nm scale

Elasticity test

The deformability index of the TEs was 14.65 ml/s with a standard deviation of 0.276. The deformability can be associated with ethanol and Tween 80 in the formulation.

Formulation and characterisation of transdermal FFG

1% TE and CL FFG was prepared using Chitosan, Propylene glycol, Oleic acid, ethanol, lactic acid and distilled water.

Evaluation of transdermal FFG of MTX

Physicochemical properties of the FFG

Table 3 indicates that both the TE and CL FFG exhibited a yellow colour, smooth texture, and uniform appearance, with the spreadability of 17.84±2.26 g/cm2 and 19.59±1.48 g/cm2, respectively, along with pH of 6.6±0.34 and 6.6±0.28 respectively. The pH of the prepared gel fell within the skin pH range, so skin irritation would not occur. The drug content of the TE FFG and CL EFG was found to be 74.45% and 80.38%, respectively.

Viscosity

The viscosity of the film-forming gel was measured using the Brookfield viscometer at 3 rpm. A comparison of the viscosity between the methotrexate-loaded transethosomal and conventional film-forming gel is presented in table 3. The viscosity of TE FFG was slightly higher than CL FFG, which may be due to the presence of the vesicle.

Table 3: Physicochemical properties and drug content of the CL and TE FFG

Form code	Appearance	*pH	*Spreadability (gm/cm²)	*Drug content (%)	Viscosity (3 rpm)*
CL FFG	Yellow colour, smooth	6.6±0.34	19.59±1.48	80.38	728.58±12.74
TE FFG	Yellow colour, smooth	6.6±0.28	17.84±2.26	74.45	881.80±8.60

*Data is given in mean ±SD (N=3), CL FFG: conventional film-forming gel; TE FFG: Transethosomal film-forming gel

Drug-excipient compatibility study by FTIR

FTIR analysis was carried out to understand the compatibility of various excipients with the drug. The comparative spectrum of the drug, optimised transethosomal suspension and transethosomal film-forming gel is shown in fig. 5. Most of the principal peaks of the drug were seen in the TE FFG and TE suspension spectra. It concluded that the drug is compatible with other excipients.

***In vitro* drug release study**

The *in vitro* drug release profile of CL and TE FFG of MTX is shown in fig. 6. The drug release after 24 h from the CL and TE FFG was found to be 97.90% and 62.559%, respectively. The release of the drug from transethosomes was slower than the conventional gel as the drug first diffused from the vesicles of the transethosomes, which then diffused from the gel. Also, the drug follows a sustained release pattern.

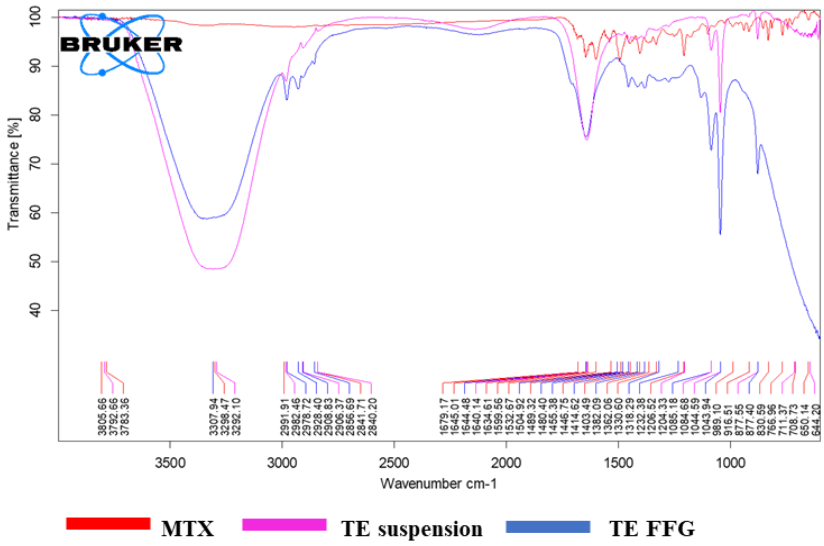

Fig. 5: Overlay of FTIR spectrum including pure MTX, optimised TE suspension and TE FFG of MTX

Various kinetic models were employed to analyse the CL and TE FFG release kinetics. Linear regression analysis was utilised to determine the drug release kinetics. The results presented in table 4 indicate that the CL FFG follows first-order drug release kinetics, whereas the TE FFG follows zero-order drug release kinetics. In addition, the Higuchi and Korsmeyer-Peppas models were employed to fit the data and understand the drug release mechanism. The R^2 (regression coefficient) value for both the gels was higher for the Higuchi model than the Korsmeyer-Peppas model. Results suggested that the drug release mechanism for both the conventional and transethosomal film-forming gels follows the Higuchi model, indicating that the drug is released through matrix diffusion.

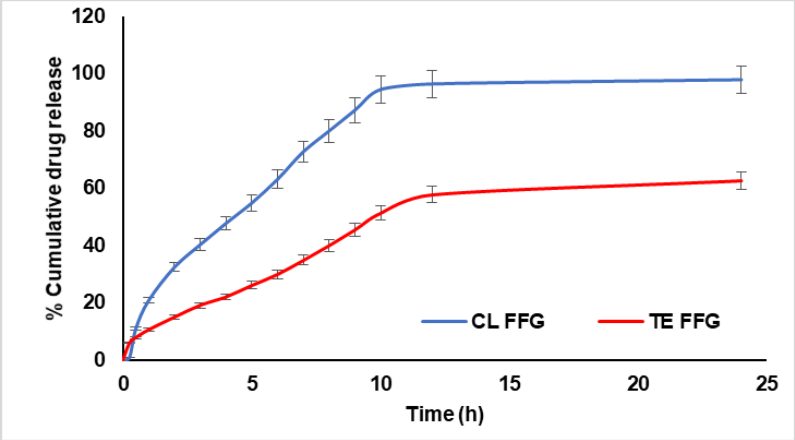

Fig. 6: Comparative *in vitro* drug release study of CL and TE FFG. Data is given in mean ±SD (N=3)

Table 4: Comparison of *in vitro* drug release kinetics

Code	Kinetic model								
	Zero-order		First order		Higuchi		Korsmeyer-peppas		
	R^2	k	R^2	k	R^2	k	R^2	k	n
CL FFG	0.9833	0.154	0.9846	-0.0012	0.9911	3.201	0.980	0.0702	0.6803
TE FFG	0.9956	0.0679	0.9955	-0.0004	0.9943	1.5282	0.9882	0.1195	0.5232

CL FFG-Conventional film-forming gel TE FFG-Transethosomal film-forming gel

Ex vivo skin permeation study using goat skin

The ex vivo study conducted for the TE FFG of MTX and the CL FFG assessed drug penetration through goat skin. As shown in fig. 7, the study conducted for 24 h showed permeation of 2147.71µg/cm² for TE FFG, which was comparatively higher than the CL FFG, which was found to be 1280.49µg/cm² for the drug. Further, the steady-state flux of TE FFG was 1.55 times greater than that of the conventional gel, as shown in table 5. This indicates a synergistic effect among the phospholipid composition of the vesicles, ethanol, and skin lipids. The enhanced drug penetration can be attributed to ethanol characteristics of fluidising the stratum corneum, thereby facilitating the penetration of the drug.

Moreover, the presence of ethanol increases the fluidity of the lipid vesicles, rendering them more flexible. These flexible vesicles penetrate intact through the stratum corneum, reaching the deeper layers of the skin and enabling drug release through the fusion of TE with skin lipids. Since the drug has to diffuse through the actual biological membrane primarily, the percentage of drug release in *ex vivo* permeation study of TE FFG was found to be lower when compared to the *in vitro* study.

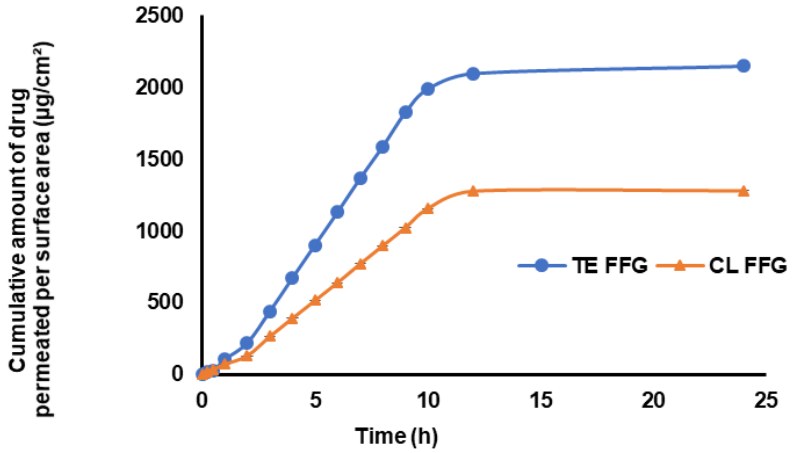

Fig. 7: Ex vivo skin permeation study of CL and TE FFG through goat skin

Table 5: The permeated amount of MTX at 24 h, flux, permeability coefficient value

Formulation code	Permeated amount at 24 h (µg/cm²)	Flux (µg/cm². h)	Permeability coefficient (Kp) x 10^{-2}(cm/h)
CL FFG	1280.49	120.36	1.20
TE FFG	2147.71	186.97	1.86

Skin irritation study

The skin irritation test was conducted on wistar rats for both blank and MTX-containing TE FFG. The results shown in fig. 8, A, and B show the control group at 0 h and 24 h, respectively, whereas fig. 8C and 8D show the test group at 0 h and 24 h, respectively. The images demonstrate that the rats did not exhibit skin irritation or erythema. This confirms the safety of the TE FFG for application on the skin.

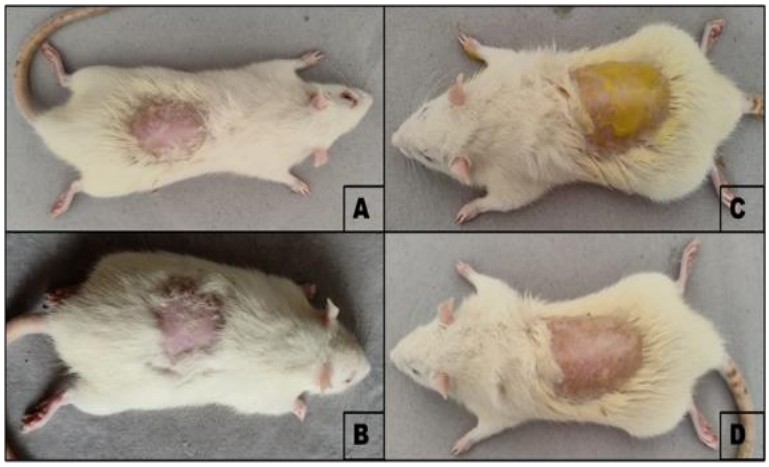

Fig. 8: Skin irritation test results: A and C show the control group and test group, respectively, at 0 hr, where B and D represent rat skin after 24 h where no sign of redness or erythema

The anti-rheumatic activity of MTX-loaded TE FFG

Swelling in the paws, along with regular monitoring of body weight changes, was a key indicator of disease advancement and an assessment of the effectiveness of anti-rheumatoid medication.

Body weight

As shown in table 6, the body weight of CFA-treated rats in arthritic Groups II–V showed a significant decrease until day seven compared to the non-arthritic group. The group treated with MTX-marketed gel and MTX-loaded TE FFG weight value was found to be increased and returned to normal levels on day 21. Further, it was noticed that the MTX-loaded TE FFG group had insignificant differences on 21 d on their zero-day compared to the marketed gel. The animals in both the non-treated arthritic group and the blank TE FFG group continued to a gradual reduction in body weight.

Paw thickness

Paw edema is another preclinical characteristic of RA, and assessing the paw edema over time indicates the disease progression. An increase in paw thickness was observed in all groups on day 7. The group treated with MTX-marketed gel and MTX-loaded TE FFG showed a gradual decrease in paw thickness on day 14, which was significant on day 21 in table 7.

Table 6: Effect of different formulations on body weight in CFA-induced arthritis model

S. No.	Group	Day 0	Day 7	Day 14	Day 21
1	Normal control	195.94±2.34	196.84±2.21	196.54±3.27	197.91±2.32
2	Disease control	204.52±2.54	195.63±3.32	187.22±3.10^{b}	181.64±3.02^{b}
3	Blank TE FFG	202.56±3.23	196.82±1.43	189.72±2.43^{*a}	182.55±2.71^{*a}
4	MTX marketed gel	199.04±2.03	189.15±1.09	192.82±2.61	194.71±3.89^{*b}
5	MTX loaded TE FEG	202.72±3.32	188.64±2.69	195.39±3.55	199.04±3.46^{*bc}

*Data is given in mean ±SD (N=5). *p<0.01 highly significant–as compared with normal control group of animals; a-p<0.05–significant, b-p<0.01 highly significant–as compared with arthritic control group of animals; c-p<0.05–significant as compared to marketed gel with transethosomal gel

Table 7: Effect of different formulations on paw thickness in CFA-induced arthritis model

S. No.	Group	Day 0	Day 7	Day 14	Day 21
1	Normal control	1.03±0.0031	1.05±0.0013	1.06±0.0061	1.04±0.0032
2	Disease control	1.13±0.0045	1.23±0.0020	1.27±0.0052*	1.31±0.0013*
3	Blank TE FFG	1.08±0.0038	1.19±0.0024	1.21±0.0076^{*a}	1.25±0.0024^{*a}
4	MTX marketed gel	1.05±0.0024	1.12±0.0014	1.10±0.0057^{*b}	1.06±0.0015^{*b}
5	MTX-loaded TE FFG	1.09±0.0021	1.18±0.0023	1.15±0.0072^{*bc}	1.11±0.0017^{*bc}

Data is given in mean ±SD (N=5). *p<0.01 highly significant–as compared with normal control group of animals; a-p<0.05–significant, b-p<0.01 highly significant–as compared with arthritic control group of animals; c-p<0.01–highly significant as compared to marketed gel with transethosomal gel

Histopathology study

From fig. 9, it can be concluded that the histopathology of synovial tissue from the ankle joints of disease-control rats showed the presence of inflammatory cells and synovitis, while the normal control rats in which no disease was induced showed the presence of fats, fibromuscular tissue, fibro collagenous tissue with no inflammatory cells. The group treated with blank TE FFG exhibited inflammatory cells in the synovial tissue. In contrast, the group treated with MTX-loaded TE FFG showed a reduction in the presence of inflammatory cells. This provided evidence of induction of disease by CFA and improved conditions by applying MTX-loaded TE FFG.

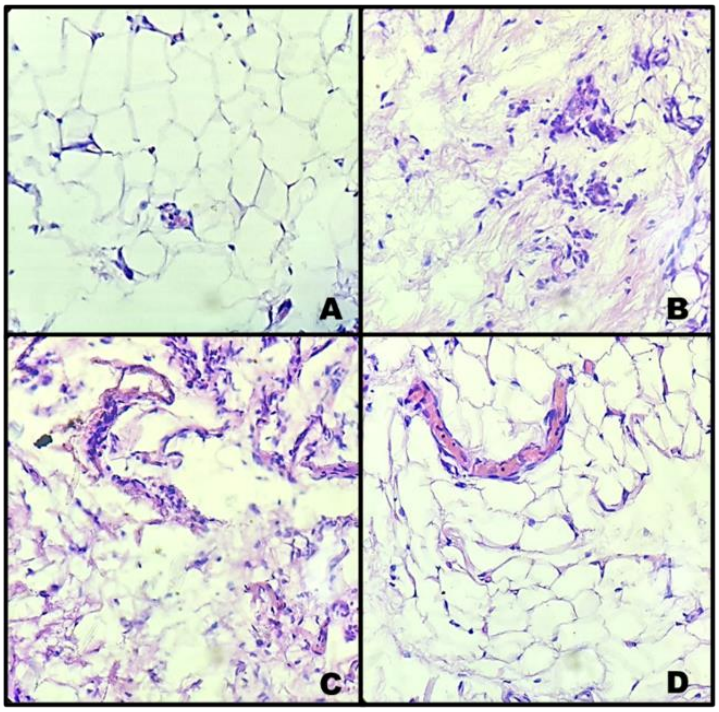

Fig. 9: Histopathology of the joint of rat belonging to A) Normal control group showing no change in the histopathology of bone B) Arthritis control group showing the presence of inflammatory cells and synovitis C) Blank TE group also showing the presence of inflammatory cells in the synovial tissue. D) MXT-loaded TE FFG treated group distinguished by the significantly lesser and minimal presence of inflammatory cells. Magnified view in 400X

CONCLUSION

The TE containing MTX was successfully prepared using the thin film method using different concentrations of soya lecithin, surfactant, and ethanol according to the Box Behnken design. The optimised transethosomes were uniform and spherical. The TE FFG had a high permeation capacity compared to the CL FFG. The histopathology results showed that the MTX-loaded TE FFG group showed a reduction and minimal presence of inflammatory cells. Moreover, it was proved that it serves as a promising approach for the effective treatment of RA by enhancing the therapeutic efficacy of MXT while minimising oral and systemic side effects.

ACKNOWLEDGEMENT

The authors thank the NGSM Institute of Pharmaceutical Sciences, Mangalore, for providing the necessary research facilities. The authors also thank ICON Labs, Navi Mumbai, for performing the TEM analysis.

FUNDING

The project does not have any external funding

AUTHORS CONTRIBUTIONS

Poojari Pratiksha N: Concept, Literature Search, Materials and Design, Data Collection, Processing, Analysis and/or Interpretation, Writing; Sneh Priya: Concept, Resources, Materials, Design, Supervision, Analysis and/or Interpretation, Writing, Critical Reviews; Sanjana: Data Collection, Processing, Analysis and/or Interpretation; Prasanna Shama Khandige: Supervision, Writing, Critical Reviews

CONFLICT OF INTERESTS

The authors declared no conflict of interest.

REFERENCES

1. Radu AF, Bungau SG. Management of rheumatoid arthritis: an overview. Cells. 2021 Oct 23;10(11):2857. doi: 10.3390/cells10112857, PMID 34831081.
2. Ahuja NK, Rajawat JS. Novel nano therapeutic materials for the effective treatment of rheumatoid arthritis recent insights. Int J App Pharm. 2021;13(6):31-40. doi: 10.22159/ijap.2021v13i6.42912.
3. Zhao Z, Hua Z, Luo X, LI Y, YU L, LI M. Application and pharmacological mechanism of methotrexate in rheumatoid arthritis. Biomed Pharmacother. 2022 Jun 1;150:113074. doi: 10.1016/j.biopha.2022.113074, PMID 35658215.
4. Vezmar S, Becker A, Bode U, Jaehde U. Biochemical and clinical aspects of methotrexate neurotoxicity. Chemotherapy. 2003 May 7;49(1-2):92-104. doi: 10.1159/000069773, PMID 12714818.
5. Murakami T, Mori N. Involvement of multiple transporters mediated transports in mizoribine and methotrexate pharmacokinetics. Pharmaceuticals (Basel). 2012 Aug 10;5(8):802-36. doi: 10.3390/ph5080802, PMID 24280676.
6. Wang X, Yan H. Methotrexate loaded porous polymeric adsorbents as oral sustained release formulations. Mater Sci Eng C Mater Biol Appl. 2017 Sep 1;78:598-602. doi: 10.1016/j.msec.2017.04.136, PMID 28576027.
7. Das S, Sharadha M, Venkatesh MP, Sahoo S, Tripathy J, Gowda DV. Formulation and evaluation of topical nanoemulgel of methotrexate for rheumatoid arthritis. Int J App Pharm. 2021;13(5):351-7. doi: 10.22159/ijap.2021v13i5.41026.
8. Mazzaferro S, Bouchemal K, Ponchel G. Oral delivery of anticancer drugs I: General considerations. Drug Discov Today. 2013 Jan 1;18(1-2):25-34. doi: 10.1016/j.drudis.2012.08.004, PMID 22951365.
9. Prasad R, Koul V. Transdermal delivery of methotrexate: past present and future prospects. Ther Deliv. 2012 Mar;3(3):315-25. doi: 10.4155/tde.12.3, PMID 22833992.
10. Jalajakshi MN, Chandrakala V, Srinivasan S. An overview: recent development in transdermal drug delivery. Int J Pharm Pharm Sci. 2022;14(10):1-9, doi: 10.22159/ijpps.2022v14i10.45471.
11. Srinivas PS, Babu DR. Formulation and evaluation of parenteral methotrexate nanoliposomes. Int J Pharm Pharm Sci. 2014;6(11):295-300.
12. Ferrara F, Benedusi M, Cervellati F, Sguizzato M, Montesi L, Bondi A. Dimethyl fumarate loaded transethosomes: a formulative study and preliminary ex vivo and *in vivo*

evaluation. Int J Mol Sci. 2022 Aug 6;23(15):8756. doi: 10.3390/ijms23158756, PMID 35955900.
13. Abdallah MH, Elghamry HA, Khalifa NE, Khojali WM, Khafagy ES, Shawky S. Development and optimization of erythromycin loaded transethosomes cinnamon oil based emulgel for antimicrobial efficiency. Gels. 2023 Feb 6;9(2):137. doi: 10.3390/gels9020137, PMID 36826307.
14. Albash R, Abdelbary AA, Refai H, El-Nabarawi MA. Use of transethosomes for enhancing the transdermal delivery of olmesartan medoxomil: *in vitro* ex vivo and *in vivo* evaluation. Int J Nanomedicine. 2019 Mar15;14:1953-68. doi: 10.2147/IJN.S196771, PMID 30936696.
15. Kaur PR, Garg VA, Bawa PA, Sharma RO, Singh SK, Kumar BI. Formulation systematic optimisation *in vitro* ex vivo and stability assessment of transethosome based gel of curcumin. Asian J Pharm Clin Res. 2018;11(2):41-7. doi: 10.22159/ajpcr.2018.v11s2.28563.
16. Aprianti I, Iskandarsyah SH, Setiawan H. Diflunisal transethosomes for transdermal delivery: formulation and characterisation. Int J App Pharm. 2023;15(3):61-6. doi: 10.22159/ijap.2023v15i3.47691.
17. Ascenso A, Raposo S, Batista C, Cardoso P, Mendes T, Praça FG. Development characterization and skin delivery studies of related ultradeformable vesicles: transfersomes ethosomes and transethosomes. Int J Nanomedicine. 2015 Sep 18;10:5837-51. doi: 10.2147/IJN.S86186, PMID 26425085.
18. N Politis S, Colombo P, Colombo G, M Rekkas D. Design of experiments (DoE) in pharmaceutical development. Drug Dev Ind Pharm. 2017 Jun 3;43(6):889-901. doi: 10.1080/03639045.2017.1291672, PMID 28166428.
19. Vanaja K, Shobha Rani RH. Design of experiments: concept and applications of plackett burman design. Clin Res Regul Aff. 2007 Jan 1;24(1):1-23. doi: 10.1080/10601330701220520.
20. Decaestecker TN, Lambert WE, Van Peteghem CH, Deforce D, Van Bocxlaer JF. Optimization of solid phase extraction for a liquid chromatographic tandem mass spectrometric general unknown screening procedure by means of computational techniques. J Chromatogr A. 2004 Nov 12;1056(1-2):57-65. doi: 10.1016/j.chroma.2004.06.010, PMID 15595533.
21. Fukuda IM, Pinto CF, Moreira CS, Saviano AM, Lourenço FR. Design of experiments (DoE) applied to pharmaceutical and analytical quality by design (QbD). Braz J Pharm Sci. 2018 Nov 8;54:e01006. doi: 10.1590/s2175-97902018000001006.
22. Zeb A, Qureshi OS, Kim HS, Cha JH, Kim HS, Kim JK. Improved skin permeation of methotrexate via nanosized ultradeformable liposomes. Int J Nanomedicine. 2016 Aug 8;11:3813-24. doi: 10.2147/IJN.S109565, PMID 27540293.
23. Nayak D, Tawale RM, Aranjani JM, Tippavajhala VK. Formulation optimization and evaluation of novel ultra deformable vesicular drug delivery system for an anti-fungal drug. AAPS Pharm Sci Tech. 2020 May 17;21(5):140. doi: 10.1208/s12249-020-01681-5.
24. Guimaraes D, Noro J, Loureiro A, Lager F, Renault G, Cavaco Paulo A. Increased encapsulation efficiency of methotrexate in liposomes for rheumatoid arthritis therapy. Biomedicines. 2020 Dec 1;8(12):1-15. doi: 10.3390/biomedicines8120630, PMID 33353028.
25. Habib BA, Sayed S, Elsayed GM. Enhanced transdermal delivery of ondansetron using nanovesicular systems: fabrication characterization optimization and ex-vivo permeation study-box-cox transformation practical example. Eur J Pharm Sci. 2018 Mar 30;115:352-61. doi: 10.1016/j.ejps.2018.01.044.
26. Hassan AS, Hofni A, Abourehab MA, Abdel Rahman IA. Ginger extract loaded transethosomes for effective transdermal permeation and anti-inflammation in rat model. Int J Nanomedicine. 2023;18:1259-80. doi: 10.2147/IJN.S400604, PMID 36945254.
27. Rady M, Gomaa I, Afifi N, Abdel Kader M. Dermal delivery of Fe-chlorophyllin via ultra deformable nanovesicles for photodynamic therapy in melanoma animal model. Int J Pharm. 2018 Sep 5;548(1):480-90. doi: 10.1016/j.ijpharm.2018.06.057, PMID 29959090.
28. Khasraghi AH, Vartanian L, Thomas LM. Preparation and evaluation of lornoxicam film forming gel. Drug Invent Today. 2019 Aug 1;11(8):1906-13.
29. Shetty S, Jose J, Kumar L, Charyulu RN. Novel ethosomal gel of clove oil for the treatment of cutaneous candidiasis. J Cosmet Dermatol. 2019 Jun 1;18(3):862-9. doi: 10.1111/jocd.12765, PMID 30171656.
30. Hegdekar NY, Priya S, Shetty SS, Jyothi D. Formulation and evaluation of niosomal gel loaded with asparagus racemosus extract for anti-inflammatory activity. Ind J Pharm Edu Res. 2023 Jan 1;57(1s):s63-74. doi: 10.5530/ijper.57.1s.8.
31. Avasatthi V, Pawar H, Dora CP, Bansod P, Gill MS, Suresh S. A novel nanogel formulation of methotrexate for topical treatment of psoriasis: optimization *in vitro* and *in vivo* evaluation. Pharm Dev Technol. 2016 Jul 3;21(5):554-62. doi: 10.3109/10837450.2015.1026605, PMID 26024238.
32. Maru AD, Lahoti SR. Formulation and evaluation of moisturising cream containing sunflower wax. Int J Pharm Pharm Sci. 2018 Nov 1;10(11):54-9. doi: 10.22159/ijpps.2018v10i11.28645.
33. Raychaudhuri R, Pandey A, Das S, Nannuri SH, Joseph A, George SD. Nanoparticle impregnated self-supporting protein gel for enhanced reduction in oxidative stress: a molecular dynamics insight for lactoferrin polyphenol interaction. Int J Biol Macromol. 2021 Oct 31;189:100-13. doi: 10.1016/j.ijbiomac.2021.08.089, PMID 34411613.
34. Jain A, Jain SK. *In vitro* release kinetics model fitting of liposomes: an insight. Chem Phys Lipids. 2016 Dec 1;201:28-40. doi: 10.1016/j.chemphyslip.2016.10.005, PMID 27983957.
35. Kotian V, Koland M, Mutalik S. Nanocrystal based topical gels for improving wound healing efficacy of curcumin. Crystals. 2022 Nov 1;12(11):1565. doi: 10.3390/cryst12111565.
36. Parhi R, Panchamukhi T. RSM-based design and optimization of transdermal film of ondansetron HCl. J Pharm Innov. 2020 Mar 1;15(1):94-109. doi: 10.1007/s12247-019-09373-9.
37. Ghosh S, Mukherjee B, Chaudhuri S, Roy T, Mukherjee A, Sengupta S. Methotrexate aspasomes against rheumatoid arthritis: optimized hydrogel loaded liposomal formulation with *in vivo* evaluation in wistar rats. AAPS Pharm Sci Tech. 2018 Apr 1;19(3):1320-36. doi: 10.1208/s12249-017-0939-2, PMID 29340978.
38. Subongkot T, Duangjit S, Rojanarata T, Opanasopit P, Ngawhirunpat T. Ultradeformable liposomes with terpenes for delivery of hydrophilic compound. J Liposome Res. 2012 Sep;22(3):254-62. doi: 10.3109/08982104.2012.690158, PMID 22663352.
39. Zafar A, Alruwaili NK, Imam SS, Yasir M, Alsaidan OA, Alquraini A. Development and optimization of nanolipid based formulation of diclofenac sodium: *in vitro* characterization and preclinical evaluation. Pharmaceutics. 2022 Mar 1;14(3):507. doi: 10.3390/pharmaceutics14030507.
40. Zhao L, Temelli F, Curtis JM, Chen L. Preparation of liposomes using supercritical carbon dioxide technology: effects of phospholipids and sterols. Food Res Int. 2015 Nov 1;77:63-72. doi: 10.1016/j.foodres.2015.07.006.
41. Khalid H, Batool S, Din F. Macrophage targeting of nitazoxanide loaded transethosomal gel in cutaneous leishmaniasis. R Soc Open Sci. 2022 Oct 5;9(10). doi: 10.1098/rsos.220428.
42. El-Menshawe SF, Ali AA, Halawa AA, Srag El-Din AS. A novel transdermal nanoethosomal gel of betahistine dihydrochloride for weight gain control: *in vitro* and *in vivo* characterization. Drug Des Devel Ther. 2017 Nov 28;11:3377-88. doi: 10.2147/DDDT.S144652, PMID 29238164.